

Interferometer for variable astrophysical radio sources

Jānis Šteinbergs¹,^{a,*} Karina Šķirmante¹,^a Artis Aberfelds¹,^a
Vladislavs Bezrukovs¹,^a Ivar Shmeld,^a and Ross A. Burns¹,^{a,b}

^aVentspils University of Applied Sciences, Engineering Research Institute

“Ventspils International Radio Astronomy Centre,” Ventspils, Latvia

^bRIKEN Cluster for Pioneering Research, Saitama, Japan

ABSTRACT. With the recent observational confirmation of accretion bursts in high-mass protostars, high-mass star formation has entered the discipline of time-domain astronomy. These bursts of accretion cause variations in the radio continuum emission and radio frequency maser emission emitted by these protostars, but the causes and mechanisms by which these variations arise have yet to be explored exhaustively. The associated rising demand for high-cadence observations calls for the development of observational facilities that can effectively monitor the radio frequency continuum and maser emission in a manner that provides high detection sensitivity and can be highly automated. We have initiated the Interferometer for Variable Astrophysical Radio Sources (IVARS) project, which comprises the development of an 800-m single-baseline radio interferometer, along with highly automated observation and data processing infrastructure, to monitor a sample of 30 high-mass protostars. We describe the project background and automation tools developed as part of the IVARS project.

© The Authors. Published by SPIE under a Creative Commons Attribution 4.0 International License. Distribution or reproduction of this work in whole or in part requires full attribution of the original publication, including its DOI. [DOI: [10.1117/1.JATIS.11.1.018001](https://doi.org/10.1117/1.JATIS.11.1.018001)]

Keywords: maser; star formation; interferometry; automatic data processing

Paper 24086G received Jun. 16, 2024; revised Dec. 12, 2024; accepted Dec. 13, 2024; published Jan. 16, 2025.

1 Introduction

1.1 Scientific Background

The study of the high-mass star forming (HMSF) remains an active area of investigation within modern astrophysics, with a focus on understanding the process by which these stars achieve their exceptionally large final masses (for review see, e.g., Ref. 1). The accretion process, once thought to be steady in nature, is now thought to likely be episodic in nature, where long periods of low-rate accretion are punctuated by short bursts of intense accretion. A prominent indicator in this research is the detection of molecular maser emission, particularly the methanol 6.7-GHz maser emission,² which is believed to manifest during the early stages of protostellar evolution, with many associated with protostellar discs.^{3,4} As this particular maser transition is pumped by infrared emission, which is emitted during accretion, this maser has proven to be a valuable tool for identifying and investigating accretion bursts in high-mass protostars.

However, the presence of maser radiation from a star’s disk is not the sole evidence of ongoing processes during star formation. Instances of accretion bursts from the protostellar disc also lead to changes in the protostar’s radio continuum emission. The first recorded accretion burst event in a still-forming high-mass star occurred in 2016,⁵ characterized by intense radio

*Address all correspondence to Jānis Šteinbergs, janis.steinbergs@venta.lv

wavelength maser emission alongside a decrease in the overall radio brightness of the protostar due to the expansion of the stellar surface radius.⁶ The identification of this phenomenon, occurring on days to years timescales, revitalized the study of high-mass star formation astrophysics, transforming it into a dynamic field of astronomy where time-dependent observations are needed. At present, radio telescopes are actively scouring the sky for additional accretion burst events. Since 2016, four such events have been identified based on their heightened brightness.^{5,7–9}

The observational hunt for these events raises new challenges. High-cadence observations with sensitivity to changes in the weak milli jansky radio continuum emission are needed. Single-baseline radio interferometers with baselines extending up to kilometers offer distinct advantages for advancing research in this burgeoning field. Compared with single-dish radio telescopes, interferometers possess greater sensitivity to radio continuum emission due to several factors.

First, all radio telescopes have an inherent system noise, which determines the signal-to-noise ratio of detection in an observation. As the system noise of each telescope is independent and random, they do not correlate, leading to an improvement of $\sqrt{2}$ during cross-correlation compared with a single-dish telescope of equivalent surface area. This gives the equivalent benefit as would be gained from doubling the frequency bandwidth or integration time. In the case of a single-dish telescope, this improvement would be equivalent to a 19% increase in the telescope aperture diameter.

Second, as radio telescopes average all signals falling within the primary beam, the beam dilution factor further degrades the signal-to-noise when sources are small compared with the beam size. This is evaluated as: $f_{\text{dilution}} = \Omega_{\text{source}}/\Omega_{\text{beam}}$, where Ω_{source} is the source solid angle, and Ω_{beam} is the telescope beam solid angle.

Moreover, in contrast to larger interferometric arrays, which primarily detect extremely compact emissions, short-baseline interferometers can capture signals from more extended emission regions, where accretion-driven variability occurs. The fraction of signal recovered by an interferometer observing a non-point-like emission is evaluated as

$$f_{\text{recovered}} = \frac{\left| \sin\left(\pi \frac{\theta_{\text{source}}}{\Delta\theta}\right) \right|}{\pi \frac{\theta_{\text{source}}}{\Delta\theta}}, \quad (1)$$

where θ_{source} is the angular size of the source and $\Delta\theta$ is the angular size of the fringe spacing of a given baseline. As can be seen, emissions on scales of $2 \times \Delta\theta$ lead to destructive interference and are completely filtered out, whereas sources with a similar angular size as the fringe spacing of the interferometer, or smaller, are well recovered while filtering out diffuse galactic radio emission and other unwanted sources of noise.

In addition, the utilization of large, multi-telescope arrays, which are widespread among the international radio astronomy research community, leads to a division of time among users. These demand-based limitations hinder the ability to conduct observations at the cadence necessary for studying high-mass protostellar accretion events, on timescales that match the variability of the investigated phenomena.

1.2 Technical Background

1.2.1 Radio telescopes in Irbene

Ventspils International Radio Astronomy Institute (VIRAC) of Ventspils University of Applied Sciences has developed an 800-m single-baseline interferometer consisting of 32-m (hereafter “RT-32”) and 16-m (hereafter “RT-16”) radio telescopes, which is sensitive to emission on angular scales of around 15 arcseconds. Irbene radio telescopes operate at a C band between 4.8 to 8.8 GHz using two identical receivers, both cryogenically cooled, which can be used for interferometry. In normal operation conditions, the RT-32 system temperature (T_{sys}) is ~ 28 to 34 K and for the RT-16 is ~ 32 to 40 K. Both antennas are involved in numerous observation projects, such as participating in the European very long baseline interferometry (VLBI) network, conducting methanol maser monitoring, participating in fast radio burst searches under the PRECISE project, monitoring active galactic nucleus (AGN) and solar activity, and providing communication services. Observations are recorded using dual, orthogonal, and circular polarizations. When conducting interferometric observations, data are digitized with a digital baseband

converter, undergo two-bit sampling, and are recorded to FlexBuff storage. 30 TB of storage capacity is available.

1.2.2 Interferometric observations

High-precision frequency synchronization and time-stamping are essential for interferometric observations. The stability of the frequency standard is typically characterized by using the Allan variance, which quantifies the frequency stability over time. In general, for VLBI, the phase error caused by frequency instability must generally remain below 1 radian. Higher observation frequencies and longer integration times demand lower Allan variance values, necessitating greater frequency stability.¹⁰

To meet these stringent requirements, we use a hydrogen atomic clock as the frequency source. In the case of Irbene radio telescopes,^{11,12} data recorded during interferometric observations are synchronized using a T4 Science Hydrogen Maser 3000, housed at the RT-16 telescope. The maser's signal is transmitted to the RT-32 telescope via the "White Rabbit" system, which utilizes an optical fiber connection to deliver the 10-MHz reference signal.^{13–15} This solution ensures minimal signal degradation during transmission. The White Rabbit technology, provided and installed by Safran Corporation, delivers a stable 10-MHz signal to the remote site with an Allan variance better than 10^{-15} over a 1-day operation period. For data time-stamping, public Network Time Protocol servers were used to ensure accurate and reliable timing.

Recorded RT-32 and RT-16 data are correlated with the Software FX Correlator (SFXC).¹⁶ providing a spectral resolution of 0.002 MHz, or a velocity spacing of 0.088 km s^{-1} at 6.7 GHz. More details on the correlation process are given in Sec. 3.4. Correlated data are processed using the Astronomical Image Processing Software (AIPS) package, which is scripted using the ParselTongue¹⁷ interface. During this stage, signal phase divergences at RT-32 and RT-16 are calibrated, in addition to applying gain calibration, enabling observations to approach the theoretical sensitivity limit of the interferometer, which is about 5.6 mJy for a 120 s integration. For comparison, the sensitivity limit of the very large array (VLA) for a similar bandwidth and integration time would be about 0.1 mJy.

More details on the data reduction pipeline are given in Sec. 3.5. The result of a pilot operation of this radio interferometer system and its data processing procedures are published in Ref. 18.

2 Source Selection

The 6.7-GHz methanol maser is widely thought to appear exclusively in the close vicinity of high-mass protostars.¹⁸ A total of 30 high-mass protostars were selected for our sample such that observations may be grouped into 10 groups (listed as groups A through J) of three targets, allowing observation procedures to be standardized for each group. This standardization facilitates the automation of all subsequent processes. Maser sources with a variety of temporal behaviors were chosen to enable the investigation of a variety of astrophysical phenomena, namely, maser flares, maser periodicity, and radio continuum detectability. The 30 targets were selected based on maser monitoring results¹⁹ (see Fig. 1) and the presence of radio continuum emission in the VLA maps of Ref. 20 (example shown in Fig. 2).

Sources were then grouped based on the proximity of their coordinates to suppress excessive slew times. Furthermore, as the sky projection of the fringe pattern of the interferometer will rotate as sources are tracked, each group was allocated a specific range in local sidereal time (LST) in which their observation may occur. This ensures that each target is always observed at the same elevation and sky position angle each time, thus avoiding any variations in the amount of resolved structure in the source emission during the monitoring campaign. The list of sources and their characteristics in these regards are given in Table 1.

To provide robust band-pass and absolute flux calibration, scans of two maser sources, W3OH and G111.542 + 0.776, and two bright continuum sources, J2202 + 4216 and J2230 + 6946, were scheduled at the beginning of the observations of all groups. These spectral line and continuum calibrator sources are considered of generally low variability in their respective domains, and all four are of sufficiently high declination that they can be observed at any time from the Irbene Radio Observatory.

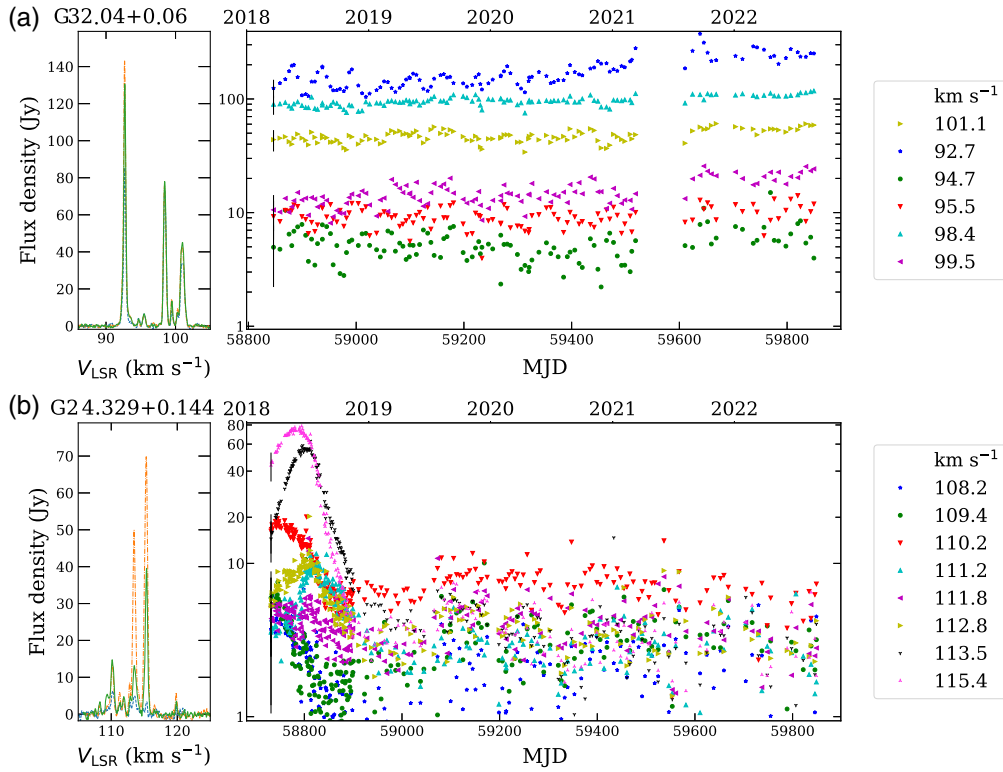


Fig. 1 Methanol maser light curve examples showing (a) flare activity in high-mass protostar G23.33 + 0.14, and (b) periodic maser variability in high-mass protostar G32.04 + 0.06, from Ref. 19. Colored points trace the time-variable flux densities of specific maser velocity components seen in the spectra on the left.

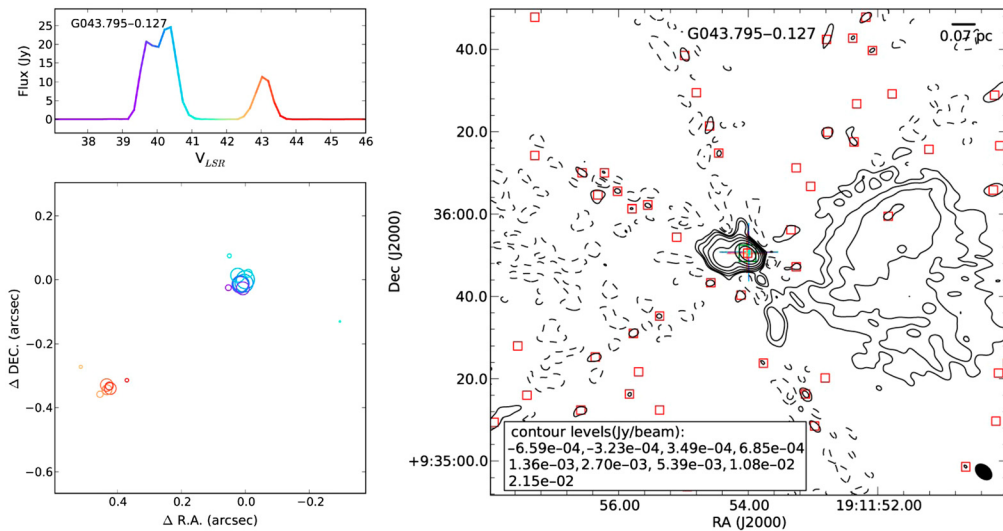


Fig. 2 Methanol maser and continuum emission in high-mass protostar G043.795 – 0.127, which is included in our survey target list, from the VLA imaging survey of Ref. 20.

3 Data Management and Flow at the Irbene Single-Baseline Interferometer

Radio interferometric observation is a complex process; it involves multiple steps. (1) Observation planning: arranging frequencies of spectral windows considering source velocity, source scan lengths, and other factors, (2) create all necessary files that are used by the telescope control

Table 1 Sources list and details.

Target name	RA (hh:mm:ss.s)	DEC (dd:mm:ss.s)	Maser (Jy)	Continuum ^a (Y/N)	Type	Group
G196.454 – 1.677	6:14:37.69	13:49:36.2	12.2	N	Periodic 110 d	A
G188.946 + 0.886	6:8:53.343	21:38:29.14	690	Y	Periodic	A
G192.599 – 0.048	6:12:54.02	17:59:23.3	85	Y	Past flare	A
G009.621 + 0.195	18:6:14.45	–201320:31:27.2	5000	Y	Periodic	B
G15.034 – 0.673	18:20:23.8	–16:11:36	13.0	Y	M17	B
G14.227 – 0.511	18:18:12.7	–16:49:33.8	1.2	—	No classification	B
G022.356 + 0.066	18:31:44.9	–9:22:5.01	37	N	Periodic (170 d)	C
G023.706 – 0.198	18:35:12.07	–8:17:49.8	17.2	Y	No classification	C
G24.33 + 0.14	18:35:8.145	–7:35:1.79	5.0	N	Flare recurring	C
G028.304 – 0.387	18:44:21.59	–4:17:33.9	15.0	Y	No classification	D
G029.955 – 0.016	18:46:3.98	–2:39:22.2	150	Y	No classification	D
G030.224 – 0.180	18:47:8.16	–2:29:42.7	16	N	No classification	D
G030.378 – 0.295	18:47:50.76	–2:24:4	8.0	N	Periodic	E
G030.817 – 0.056	18:47:46.38	–1:54:36.7	15	N	Maybe periodic	E
G31.060 + 0.092	18:47:41.62	–1:37:27.3	100	Y	W43	E
G033.641 – 0.227	18:53:32.7	0:31:50.6	120	Y	Variable and periodic	F
G034.244 + 0.133	18:53:18.5	1:14:58.4	20	Y	No classification	F
G32.744 – 0.076	18:51:21.87	0:12:5.3	45	Y	Best maser cal	F
G043.795 – 0.127	19:11:54.01	9:35:50.5	25	Y	Periodic	G
G045.472 + 0.133	19:14:8.56	11:12:26.5	5	N	Periodic	G
G049.599 – 0.249	19:23:28.93	14:40:0.8	600	N	No classification	G
G075.782 + 0.342	20:21:44.12	37:26:39.5	60	Y	No classification	H
G069.539 – 0.975	20:10:9.075	31:31:34.86	100	Y	No classification	H
G78.122 + 3.633	20:14:25.88	41:13:36.87	120	N	Active maser	H
G81.767 + 0.596	20:39:2	42:24:59.3	2	N	No classification	I
G81.8713 + 0.7807	20:38:36.425	42:37:34.56	500	Y	W75N	I
G085.410 + 0.003	20:54:13.67	44:54:8	80	Y	Past flare	I
G109.871 + 2.113	22:56:18.12	62:1:46.3	600	Y	Cepheus A	J
G108.184 + 5.518	22:28:52.1	64:13:43.4	20	N	No classification	J
G107.298 + 5.639	22:21:26.81	63:51:37.14	150	—	Periodic 34 d	J

^aDetections (where “—” indicates absence) are determined based on the presence of emission of at least one contour line in the VLA maps of Ref. 20.

system, (3) running the observations, (4) correlating data from the two telescopes, (5) processing and calibration of the interferometric data. Many of these processes can be at least somewhat automated. In this effort, the VIRAC team has created a specialized web information system, the automatic correlation system (ACor).

ACor is a web-based information system designed to facilitate observation planning, data storage, and data processing. ACor automates various processes, enhancing efficiency by predominantly executing tasks automatically. This system enables seamless integration of observational data into a structured database, streamlining the entire data management and analysis workflow.

The primary requirements for the information system include open access, web-based functionality, and the organization of observation scheduling involving researchers, radiotelescope operators, and data processing specialists. The system is designed to automate observation scheduling for both single-dish and interferometric modes using the Irbene radio telescope complex, which comprises RT-32, RT-16, and low frequency array (LOFAR) radio telescopes. In addition, the system manages the storage of observation parameters in a structured database. Furthermore, the system offers automated capabilities for autocorrelation and cross-correlation analyses, as well as a clock search for fringe findings. In the event of unsuccessful observation results, the system is equipped with automatic planning for observation rescheduling to optimize data collection efforts.

3.1 Technological Solutions Utilized in ACor Development

To meet the previously mentioned requirements, the project team opted to develop the web application as an application programming interface (API)-driven information system, allowing for a modular front-end composed of multiple solutions that can operate concurrently. The ACor system was architected as a two-tiered system comprising: (1) the back-end, predominantly implemented in Java utilizing the Spring Framework;²¹ and (2) the front-end, developed as a single-page application (SPA) using Angular and TypeScript libraries.²² This architectural choice facilitates efficient communication between the back-end servers and the front-end application. To achieve this communication, representational state transfer (REST) was employed. REST technology facilitates the transmission of JavaScript Object Notation requests and responses, enabling the straightforward creation of an API for server-client interaction. This is achieved by defining consistent endpoints using Spring Framework controllers' classes. The primary rationale for selecting Java as the back-end programming language stems from its attributes as a high-performance, object-oriented, multithreaded, open-source, and platform-independent general-purpose language. Although Java is often categorized as an interpreted language, it also employs a just-in-time compilation technique, which compiles and optimizes code during runtime. The Spring Framework, built on Java, streamlines the development process by offering built-in annotations for function mapping.

ACor leverages multiple sub-frameworks of the Spring ecosystem, such as Spring Security for security protocols and Spring Data Java Persistence API (JPA) for data management. ACor adopts the Spring Model-View-Controller pattern.²³ complemented by additional service implementations to handle the system's business logic. On the front end, ACor utilizes SPA technology to ensure mobile-friendliness and cross-device compatibility. SPAs typically offer faster performance compared with multi-page applications as their scripts are loaded only once during the application's lifecycle. Angular was chosen as the primary front-end technology due to its efficiency, performance, and increasing popularity in recent years. Research into potential technologies indicated a beneficial synergy between Spring Framework and Angular, as evidenced by their successful integration in numerous large-scale IT projects.

The ACor system utilizes the MySQL database, renowned for its efficiency, user-friendly interface, and robustness. MySQL ensures consistent uptime, which is vital for the uninterrupted operation of web-based systems such as ACor. Being open-source, MySQL offers a cost-effective solution for database management.²⁴ In addition, its compatibility with the Spring Data JPA framework facilitates seamless integration and connectivity through repository interfaces, optimizing data storage and retrieval processes within the ACor system.

3.2 ACor Database Schema: Overview of Tables and Data Management Structures

The MySQL database schema for the ACor system encompasses a comprehensive set of tables designed to manage various aspects of the observational and data processing workflows. An entity-relationship diagram of the Acor database is shown in Fig. 3, and more details on each item are given in the [Appendix](#). This schema provides a structured and organized approach to

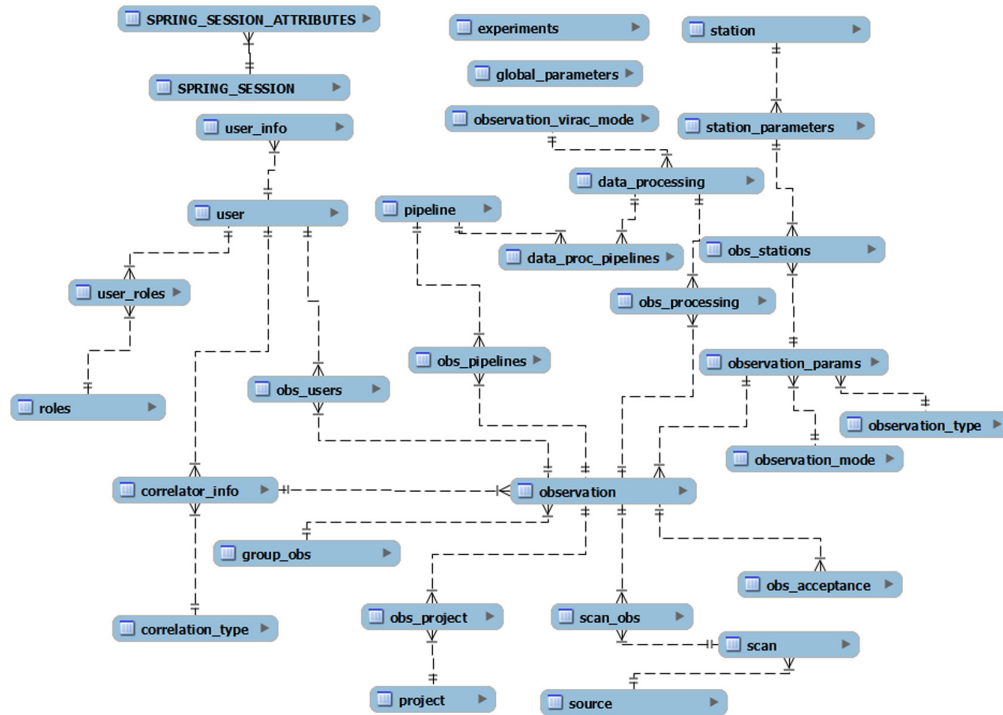


Fig. 3 Entity relation diagram of the ACor system.

data management, facilitating efficient storage, retrieval, and manipulation of data across various components of the ACor system.

When undertaking observations, first, a “key file” must be created, which is the standard format for setup and scan scheduling in VLBI observations, developed by the National Radio Astronomical Observatory.²⁵ The key file is input to the JIVE-developed tool pySCHED (<https://github.com/jive-vlbi/sched>), which creates a VEX file that is needed for the telescope control system. After that, the observation is run, and data are recorded. When data from both telescopes are obtained, they are correlated using the JIVE-developed correlator SFXC.¹⁶ After that, correlated data are processed with a custom ParselTounge pipeline developed for the Interferometer for Variable Astrophysical Radio Sources (IVARS) project. The majority of these steps are handled by the ACor system.

The VIRAC data center consists of (1) Flexbuffs—for initial data storage after observation, (2) LOFAR data server—data storage for data processing, and (3) a high-performance computer for data processing. Within the VIRAC data center, the ACor system functions are: (1) generate a key file and create VEX file for specific observation and group, (2) send VEX file to telescope operators, (3) send data from flexbuff to LOFAR data server, (4) generate files for SFXC correlation, (5) run correlations and create measurement-set and flexible image transport system (FITS) files, (6) run the ParselTounge pipeline. A basic system overview of this process, in which the ACor’s role is highlighted, is displayed in Fig. 4.

3.3 Automation of Observation Planning

The automated scheduler serves as a valuable tool for researchers engaged in monitoring observation campaigns characterized by stable or minimally varying observation parameters.

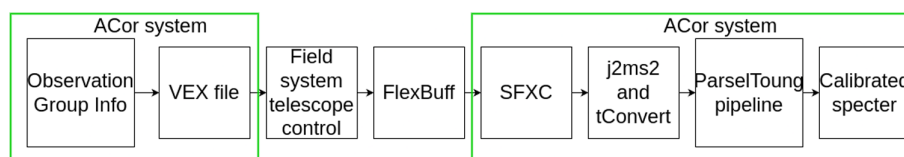


Fig. 4 Irbene single-baseline interferometer data flow overview.

As part of the IVARS project²⁶ framework, a weekly event process is initiated, activated every Monday at 9:00 AM. This process systematically reviews the predefined observation groups within the project (see Table 1, converting their LST values to Greenwich Mean Time. For assessing the availability of both antennas, RT-32 and RT-16, at specific Universal Time Coordinates (UTC) intervals, a dedicated software solution has been developed. This solution seamlessly integrates with the VIRAC observation calendar hosted on Google Calendar and an internal API-driven tool, the latter also furnishing data on other observations involving RT-16. Utilizing the aggregated data from these platforms, the automated scheduler orchestrates the creation of a new event within the VIRAC Google calendar, earmarking dedicated time slots for the respective observations. Concurrently, it compiles a VEX file aligned with the observation parameters. This VEX file is subsequently dispatched to the Flexbuff-1 server for the execution of the planned observations. In addition, the details of these observations, including their parameters and statuses, are stored in the database for record-keeping and future analysis. Following observation execution, operators annotate the VIRAC Google calendar with specific color codes to denote observation statuses: green signifies successful completion, yellow indicates partial failure with one or more scans unsuccessful, whereas red signifies comprehensive observation failure. Additional notes are appended to elucidate any encountered discrepancies or errors. The automated scheduler conducts a comprehensive review of the preceding week's observations every Monday at 8:30 AM. This review culminates in an update of the observation statuses in the database by 9:00 AM, facilitating the assessment of whether rescheduling is necessitated by any unsuccessful observations. Although manual selection of a particular group may become requisite, particularly upon the sudden emergence of an available slot in the observation schedule, the ACor system provides a feature allowing the selection of observations for execution based on antenna load and the observation's LST.

In the user interface view (see Fig. 5), the groups are configured for the specific project “IVARS,” and detailed information for each group, including the LST time and observation duration, is displayed. Users can select the date range for their desired observations. A table is generated for each day, with the first column listing specific groups, the second column showing the group's LST time, and the third and fourth columns presenting the recalculated start and end times in UTC, respectively. The fifth column indicates the observation duration in hours.

Upon loading the table, the software queries the VIRAC Google calendar for the load status of both antennas, displaying this information in the sixth and seventh columns. The eighth column provides an overview of whether interferometric observation is possible at the specified

Observation Groups

Group	Start Time (LST)	Duration (in hours)
AA, AB, AC	06:00:00	1.01667
B, C, D	16:45:00	1.93333
E, F, G	18:55:00	1.93333
H, I	21:05:00	1.91667
J	23:15:00	2.09167

Choose project

IVARS

STEF

not project

See observation possibilities

Start Date: End Date: Calculate UTC and check availability Store Observations in DB and create vex files

May 21, 2024

Group Title	Start Datetime (LST)	Start Datetime (UTC)	End Datetime (UTC)	Duration (in hours)	Availability RT-32	Availability RT-16	Observation Status	Create an Observation	Choose Group	Observation Title
AA, AB, AC	2024-05-21T06:00	2024-05-21T12:34	2024-05-21T13:35	1.01667	Unavailable	Available	NOT POSSIBLE	<input type="checkbox"/>		
B, C, D	2024-05-21T16:45	2024-05-21T23:17	2024-05-22T01:13	1.93333	Available	Available	OK	<input checked="" type="checkbox"/>	B (14)	B015
E, F, G	2024-05-21T18:55	2024-05-21T01:30	2024-05-21T03:26	1.93333	Unavailable	Available	NOT POSSIBLE	<input type="checkbox"/>		
H, I	2024-05-21T21:05	2024-05-21T03:40	2024-05-21T05:35	1.91667	Available	Available	OK	<input checked="" type="checkbox"/>	I (8)	I009
J	2024-05-21T23:15	2024-05-21T05:50	2024-05-21T07:56	2.09167	Available	Available	OK	<input checked="" type="checkbox"/>	J (1)	J002

May 22, 2024

Group Title	Start Datetime (LST)	Start Datetime (UTC)	End Datetime (UTC)	Duration (in hours)	Availability RT-32	Availability RT-16	Observation Status	Create an Observation	Choose Group	Observation Title
AA, AB, AC	2024-05-22T06:00	2024-05-22T12:30	2024-05-22T13:31	1.01667	Unavailable	Available	NOT POSSIBLE	<input type="checkbox"/>		
B, C, D	2024-05-22T16:45	2024-05-22T23:13	2024-05-23T01:09	1.93333	Available	Available	OK	<input checked="" type="checkbox"/>	B (14)	B015
E, F, G	2024-05-22T18:55	2024-05-22T01:26	2024-05-22T03:22	1.93333	Available	Available	OK	<input checked="" type="checkbox"/>	G (11)	G012
H, I	2024-05-22T21:05	2024-05-22T03:36	2024-05-22T05:31	1.91667	Available	Available	OK	<input checked="" type="checkbox"/>	I (8)	I009
J	2024-05-22T23:15	2024-05-22T05:46	2024-05-22T07:52	2.09167	Available	Available	OK	<input checked="" type="checkbox"/>	J (1)	J002

Fig. 5 ACor view of observation planning based on the groups.

time. If both antennas are available, a checkbox in the ninth column is automatically checked, although this can be manually adjusted if needed. When the checkbox in the ninth column is selected, the tenth column shows the target source group (A to J) with the fewest previous observations available at that time (by default), with the option to modify this selection as necessary.

Upon pressing the “Store Observation in DB and create vex files” button, a request is sent to the ACor backend, initiating the observation process. This process includes saving observations to the database, generating observation files, and sending them. The eleventh column displays the saved observation’s experiment code.

3.4 Automation of Correlation

The ACor system allows processing of two kinds of observation. (1) Data processing with single a scan correlation - to experiment with correlation parameters. (2) Data processing with multi-scan correlation—to run a full correlation pass of line or continuum, or both. This correlation run includes all observed scans. Multi-scan correlation uses the following correlation parameters: (1) Two second integration time, (2) In the continuum pass, all channels are correlated with 128 FFT points, (3) The line-only channel containing the maser signal is correlated with 4096 FFT points. These parameters are well suited for spectral resolution in maser observations using a 8 MHz bandwidth.

For multi-scan correlation an automatic clock search is executed. The benefits of the clock search (see Fig. 6). This is done by parsing the key file to identify the fringe finder source(s). After that it is checked if the scan witch contains the fringe finder has raw data on file. If none of the fringe finder scans have raw data files a clock search is not done. The clock search is done with 1024 FFT points, 2-s integration time and for all channels. This process is done in five iterations after the first iteration fringe mean offset value is found. If the standard deviation of the fringe offset for all channels is larger than 2, the clock search is stopped. In the next four iterations the identified fringe mean offset is subtracted and added to RT-32 GPS offset and

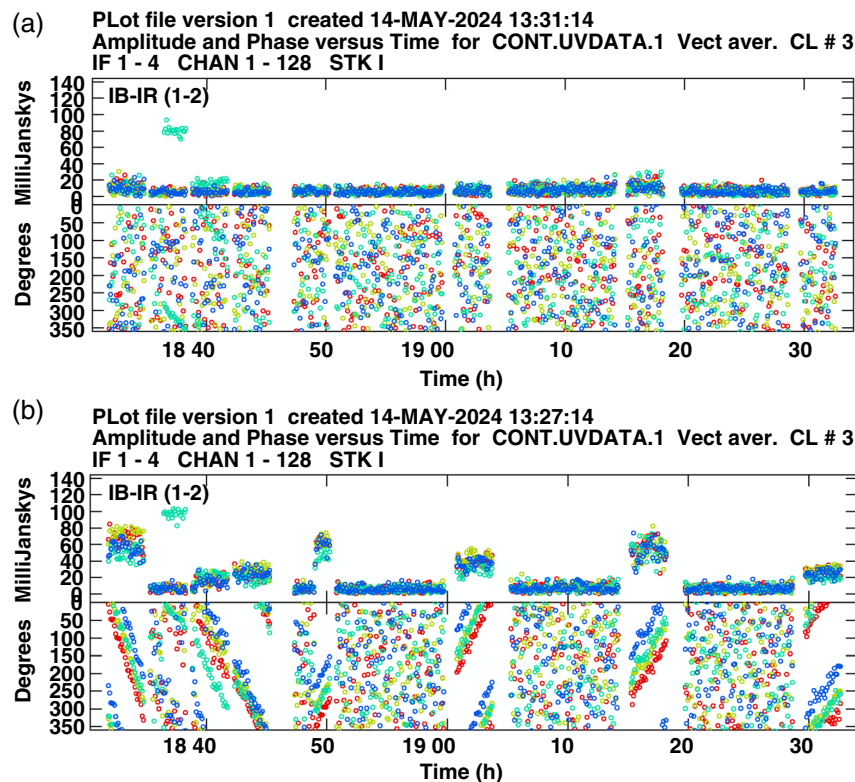


Fig. 6 Beneficial effect of the automated clock search function can be seen in the uncalibrated visibility data where previously incoherent and weakly detected sources (above) can be seen to show improved phase coherence and integrated flux density (below).

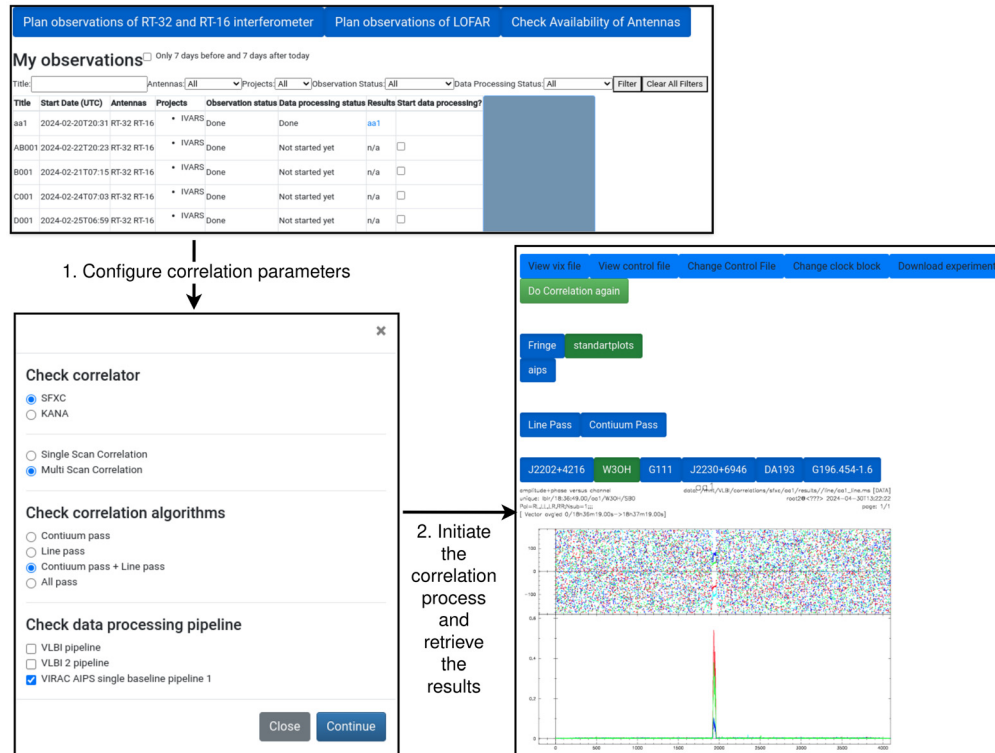


Fig. 7 ACor view of the observation data processing flow, showing a list of observations and their status, options for data processing parameters, and the results of data processing.

RT-16 GPS offset. After all iteration from all four GPS offset changes, the version where mean of fringe offset is lowest is chosen as the appropriate value for the full correlation pass.

If multi-scan correlation with both passes are done, automatic data processing is done with a ParselTounge pipeline that is described in Sec. 3.5. After the correlation “measurement set” and FITS files are created. Diagnostic plots are also created and these, in addition to the pipeline-generated diagnostic plots, are displayed to users. The overview of data processing user interface (see Fig. 7).

3.5 Automation of Data Reduction

Processing of astronomical data was standardised with the use of an automated data reduction pipeline written in ParselTounge which is a python interface to the astronomical image processing software (AIPS). The line and continuum data sets are first loaded. Beginning with the continuum data, corrections for the losses during digital sampling are applied. Then a-priori gain calibration tables (system temperature and gain curve) derived from noise diode temperature measurements conducted during observations are used to calibrate the flux density of visibilities. Bandpass corrections for all targets are made based on the observed bandpass shapes of continuum calibrators. Then, three stages of fringe fitting and integrations are performed. Starting with a “manual phase-cal” stage, the phase difference between the RCP and LCP data are corrected, and any phase delay difference between the baseband channels is corrected allowing the channels and both polarisations to be integrated to improve signal to noise. The group delay is then determined on continuum sources by fringe fitting on the partially integrated data at a solution interval of about 20 min in order to trace the slowly drifting delay differences and slowly changing phase residuals imparted by the ionosphere. Solutions are applied to all targets in the experiment. Finally the continuum sources are then fringe fitted again and in so dealing with the baseband channels individually to obtain channels specific solutions. At this stage the absolute flux scale for the experiment is fine tuned by comparison of the measured fluxes of maser and continuum calibrators, providing corrections where needed. It should be noted that all fringe fitting stages up to this point are instructed to discard phase rate solutions.

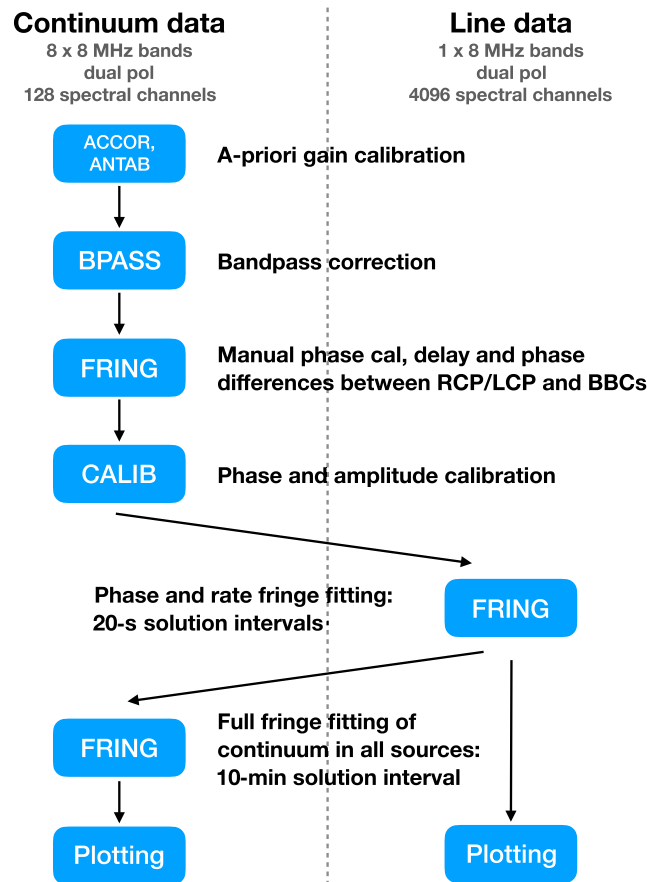


Fig. 8 Visual of the main stages of the automated AIPS data processing carried out by the ParselTongue pipeline.

At this point, the solutions for the continuum data baseband channel which matches in frequency to the line data set is copied to the line data, thus providing gain, delay and slowly changing phase solutions which can be interpolated to the timeranges of the maser target data. The peak channel of maser emission for each source is then determined and used as the input of a fringe fitting stage which determines the phase and rate fluctuations of the atmosphere with 20-s solution intervals. Phase and rate solutions are concatenated into a single solution table and copied back to the continuum data set, thus enabling long integrations aiming to detect the (typically weak) continuum emission associated with maser targets. A final fringe fitting stage is conducted on the continuum data of all targets as an inspection step as the success or failure at this stage indicates the overall detectability of continuum emission in all sources, both quasars and high-mass protostars. Finally the spectra and visibility plots of all sources are output and the integrated radio continuum flux densities of all sources determined. The overview of data reduction (see Fig. 8).

4 First Observation Results

4.1 First Results of Interferometric C Band Observation

The IVARS project operates thanks to support granted by the Latvian Science Council. As part of efforts to secure the funding grant, we performed a demonstration of the capabilities of the interferometer to confirm the feasibility of the proposed project. During this period in 2020 to 2021, observations of the methanol maser and radio continuum emission from a small sample of protostars were initiated, allowing us to begin the development and testing of our approach to observations, data processing, and automation. A sample of results from the pilot study, conducted between 2020 and 2021, is shown in Fig. 9. Small, source-inherent variations of the maser flux

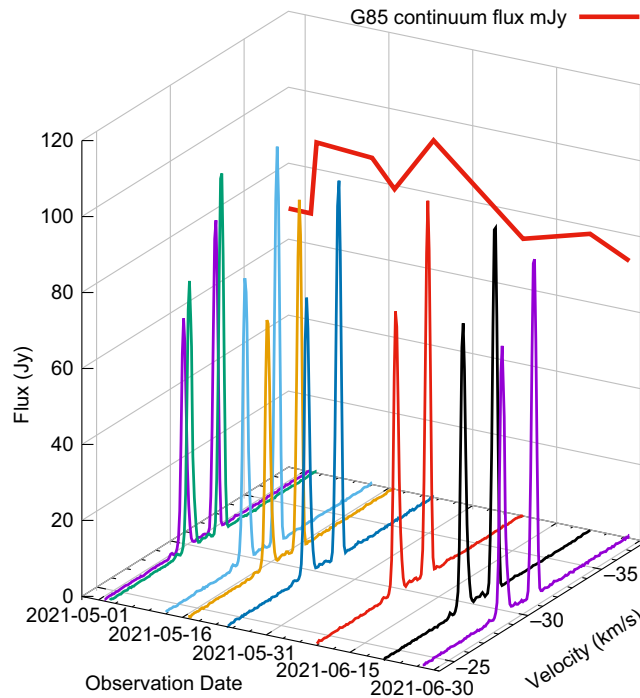


Fig. 9 Methanol maser and continuum emission in high-mass protostar G085.410 + 0.003 from pilot observations from this project.²⁷

and continuum emission can be seen, confirming the stability of gain calibration even without the use of standard flux calibrator sources, which were introduced during the post-pilot, main program.

The pilot survey confirmed that the system was operating with sufficient sensitivity and stability to deliver the scientific goals of the project. Unfortunately, in August 2021, both of the hydrogen maser clocks malfunctioned, severely jeopardizing the project. Fortunately, a new maser clock was installed at the RT-16, and the White Rabbit system was employed to revive the project. After solving other technical problems, the first successful fringe detections were achieved on February 9, 2024.

Since then, operations have been proceeding, with several small but surmountable issues being solved by the IVARS team and engineers at the Irbene Radio Observatory. In Fig. 10, we show a recently obtained example of the methanol maser and radio continuum flux

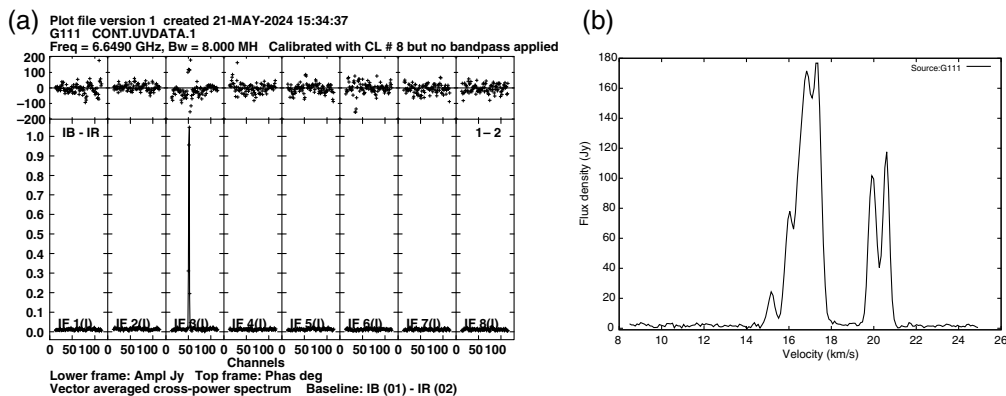


Fig. 10 Phase [upper (a)] and flux density [lower (a)] measurements for high-mass protostar G111.542 + 0.776. The maser emission seen in “IF 3” and the phase coherence across the full bandwidth demonstrate successful simultaneous measurement of the maser and radio continuum emission in high-mass protostar G111.542 + 0.776. Note that these data are from the coarse spectral resolution correlator pass, and thus, the maser amplitude is spectrally diluted. (b) Methanol maser emission from the same observation and target, from the high-resolution correlator pass.

measurements of another high-mass protostar, G111.542 + 0.776. In obtaining this result, observation scheduling, data acquisition, correlation, and data reduction were all automated. The phase stability shown in the upper left and the maser profile on the right confirm that our automated workflow is operating as planned. Thus, the revived observational system (the new maser clock in RT-16, used in conjunction with the White Rabbit solution), in addition to the software infrastructure developed by the IVARS team, is once again capable of delivering the science goals of the IVARS project. The results of our ongoing observational program will be published in a series of forthcoming papers in astronomical journals.

5 Future Works

The radio emission coming from HMSF regions tends to be quite weak, and its research and monitoring have so far often been available only to the largest radio telescopes with a diameter of 64 m and more, and compact interferometer arrays such as the Very Large Array (see for ex. Ref. 20). These telescopes are typically heavily burdened with other research, which has hindered the exploration of this radiation. The use of two relatively close small radio telescopes in the single-base interferometer mode could be a good alternative. However, so far, they have not been widely used for this purpose; thus, researchers lack the necessary experience for it. Thus, the clarification of the question of what are the possible errors and achievable accuracy of this method, as well as what are the possibilities to improve the already existing data processing methodology when using single-baseline interferometers may be of great importance.

It seems to us that a suitable way to proceed with this issue is to lean on observation simulations that take into account various instrumental and atmospheric effects and test different data processing methods using these simulations. A significant breakthrough in this area promises to be data processing methods based on radio interferometer measurement equation (RIME) (about RIME see Ref. 28). For examples of where these methods have been used for cosmic microwave background radiation (CMBR) research, see, for example, Refs. 29 and 30. Recently, software packages have been developed that allow for the simulation of the observation process and the acquisition of observation data, such as OmniUV³¹ and VieRDS.³² We plan to combine some of these packages with our developed (or improved and adapted for a single-baseline interferometer) capabilities to enhance the capabilities of our instruments for observing weak methanol and ex-OH maser sources in the 6-GHz frequency range.

6 Conclusions

The 800-m single-baseline interferometer at Irbene Radio Observatory is found to be very well suited to temporal investigations of the temporal variations in maser and radio continuum emission in high-mass protostars. This field of research is somewhat difficult to approach via the more commonly used radio observation facilities such as shared-use, high-sensitivity observatories, which cannot provide high-cadence, long-term monitoring—or single-dish observatories, which may have more availability but lack sensitivity to weak radio continuum emission. Our project, named IVARS, is undertaking this challenge by monitoring the 6.7-GHz methanol maser and radio continuum emission in a sample of 30 high-mass protostars with a roughly weekly, or better, cadence of observation.

Thanks to the reasonably short baseline length involved, the approach of a single maser clock and a system of conveying its time signal to a second radio telescope (White Rabbit) has proven to be effective and cost-efficient.

High-cadence, long-term monitoring with a reliable flux calibration procedure is greatly benefited by automation, which can assist at all stages of the workflow: scheduling, observation, correlation, and data processing. The suite of automation tools developed in the IVARS project may be utilized by other teams aiming to conduct similar observational campaigns.

Several kinds of temporal variations in maser and continuum emission in high-mass stars are known but remain largely unexplained. The continuation and wider proliferation of single-baseline radio observation campaigns provide the flexibility and sensitivity needed to deepen our understanding of the accretion, jet ejection, and other time-domain phenomena associated with the formation of massive stars.

7 Appendix: Description of the Database Tables Used for Data Storage in the ACor System

Below is an overview of the tables included in the schema 4:

- **SPRING_SESSION**: Stores session information for user interactions.
- **SPRING_SESSION_ATTRIBUTES**: Stores attributes associated with session data.
- **correlation_type**: Defines types of correlation used in data processing.
- **correlator_info**: Stores information related to correlator configurations.
- **data_proc_pipelines**: Stores data processing pipelines.
- **data_processing**: Stores details of data processing tasks.
- **global_parameters**: Stores global parameters used across the system.
- **group_obs**: Manages observational groups such as AA, AB, AC, B, C, D ... with LST time (see Table 1).
- **obs_acceptance**: Stores acceptance status of observations and is used for automatic rescheduling of observation.
- **obs_pipelines**: Stores information regarding the pipelines utilized in the specific observation.
- **obs_processing**: Stores information regarding the processing parameters used in the specific observation.
- **obs_project**: Stores information regarding which project the observation is scheduled.
- **obs_stations**: Associates stations with observations.
- **obs_users**: Manages users for observations.
- **observation**: Stores observational data.
- **observation_mode**: Defines modes of observation.
- **observation_params**: Stores parameters associated with observations.
- **observation_type**: Defines types of observations.
- **observation_virac_mode**: Manages VIRAC observation modes.
- **pipeline**: Defines data processing pipelines.
- **project**: Manages project details.
- **roles**: Defines user roles and permissions.
- **scan**: Stores scan data.
- **scan_obs**: Associates scans with observations.
- **source**: Manages source data for observations.
- **station**: Stores information about all stations.
- **station_parameters**: Stores parameters associated with observation stations.
- **user**: Manages user accounts and credentials.
- **user_info**: Stores additional information related to users.
- **user_roles**: Associates users with roles and permissions.

Disclosures

The authors have no relevant financial interests in the paper and no other potential conflicts of interest to disclose.

Code and Data Availability

The developed code is published on GitLab (https://gitlab.com/sklandrausis1/VLBI_Web_App/) and is available upon request. In acknowledgment of FAIR data availability principles, any data obtained via the IVARS project will be made available to interested parties upon reasonable request to the authors.

Acknowledgments

This publication has received funding from the Latvian Council of Science project “A single-baseline radio interferometer in a new age of transient astrophysics (IVARS)” (Grant No. lzp-2022/1-0083). We extend our thanks to the referees for constructive comments on improving this paper.

References

1. H. Zinnecker and H. W. Yorke, “Toward understanding massive star formation,” *Annu. Rev. Astron. Astrophys.* **45**, 481–563 (2007).
2. K. M. Menten, “The discovery of a new, very strong, and widespread interstellar methanol maser line,” *Astrophys. J. Lett.* **380**, L75 (1991).
3. A. J. Walsh et al., “Studies of ultracompact HII regions—II. High-resolution radio continuum and methanol maser survey,” *Mon. Not. R. Astron. Soc.* **301**, 640–698 (1998).
4. D. J. van der Walt, A. M. Sobolev, and H. Butner, “Inferences from the kinematic properties of 6.7 GHz methanol masers,” *Astron. Astrophys.* **464**(3), 1015–1022 (2007).
5. A. Caratti o Garatti et al., “Disk-mediated accretion burst in a high-mass young stellar object,” *Nat. Phys.* **13**, 276–279 (2017).
6. C. L. Brogan et al., “The extraordinary outburst in NGC6334I-MM1: dimming of the hypercompact HII region and destruction of water masers,” in *Astrophys. Masers: Unlocking the Mysteries of the Universe*, A. Tarchi, M. J. Reid, and P. Castangia, Eds., Vol. **336**, pp. 255–258 (2018).
7. T. R. Hunter et al., “An extraordinary outburst in the massive protostellar system NGC6334I-MM1: quadrupling of the millimeter continuum,” *ApJ* **837**, L29 (2017).
8. B. Stecklum et al., “Infrared observations of the flaring maser source G358.93-0.03. SOFIA confirms an accretion burst from a massive young stellar object,” *A&A* **646**, A161 (2021).
9. E. Proven-Adzri et al., “Discovery of periodic methanol masers associated with G323.46-0.08,” *Mon. Not. R. Astron. Soc.* **487**, 2407–2411 (2019).
10. L. Wang, Q. Liu, and Y. Cai, “The time and frequency system of the Tianma 65 m radio telescope,” *Astron. Tech. Instrum.* **1**, 260–266 (2024).
11. V. Bezrukovs, “Time and frequency synchronization on the VIRAC radio telescope RT-32,” *Latvian J. Phys. Tech. Sci.* **53**, 14–19 (2016).
12. P. Krehlik et al., “Fibre-optic delivery of time and frequency to VLBI station,” *A&A* **603**, A48 (2017).
13. P. Boven, “DWDM stabilized optics for white rabbit,” in *Eur. Freq. and Time Forum (EFTF)*, pp. 213–216 (2018).
14. S. Schediwy et al., “Phase synchronization for the mid-frequency square kilometre array telescope,” in *Amer. Astron. Soc. Meet. Abstracts*, Vol. 231, p. 215.03 (2018).
15. S. W. Schediwy et al., “The mid-frequency square kilometre array phase synchronisation system,” *Publ. Astron. Soc. Australia* **36**, e007 (2019).
16. A. Keimpema et al., “The SFXC software correlator for very long baseline interferometry: algorithms and implementation,” *Exp. Astron.* **39**, 259–279 (2015).
17. M. Kettenis et al., “ParselTongue: AIPS talking Python,” in *Astron. Data Anal. Softw. and Syst. XV*, C. Gabriel et al., Eds., Vol. 351, p. 497 (2006).
18. S. L. Breen et al., “Confirmation of the exclusive association between 6.7-GHz methanol masers and high-mass star formation regions,” *Mon. Not. R. Astron. Soc.* **435**, 524–530 (2013).
19. A. Aberfelds et al., “Five years of 6.7-GHz methanol maser monitoring with Irbene radio telescopes,” *Mon. Not. R. Astron. Soc.* **526**(4), 5699–5714 (2023).
20. B. Hu et al., “On the relationship of UC HII regions and class II methanol masers. I. Source catalogs,” *ApJ* **833**, 18 (2016).
21. M. Lui et al., *Introduction to Core Spring Framework*, pp. 61–101, Apress, Berkeley, California (2011).
22. G. Gunasekar et al., “Interpretation and analysis of angular framework,” in *Int. Conf. Power, Energy, Control and Transmission Syst. (ICPECTS)*, pp. 1–6 (2022).
23. A. Singh et al., “Formulating an MVC framework for web development in Java,” in *2nd Int. Conf. Tr. in Electron. and Inform. (ICOEI)*, pp. 926–929 (2018).
24. C. Györfödi et al., “Performance analysis of NOSQL and relational databases with couchDB and mySQL for application’s data storage,” *Appl. Sci.* **10**, 8524 (2020).
25. R.C. Walker, “The Sched User Manual,” <https://www.aoc.nrao.edu/software/sched/> (2023).
26. About project IVARS, <https://en.virac.eu/petnieciba/projekti/ivars>.
27. J. Šteinbergs et al., “Single-baseline interferometer for mJy observations,” in *Eur. VLBI Netw. Mini-Symp. and Users’ Meet. 2021*, PoS (2022).
28. O. M. Smirnov, “Revisiting the radio interferometer measurement equation. I. A full-sky Jones formalism,” *A&A* **527**, A106 (2011).
29. A. Karakci et al., “Bayesian inference of polarized cosmic microwave background power spectra from interferometric data,” *ApJS* **204**, 10 (2013).

30. A. Lewis, A. Challinor, and A. Lasenby, “Efficient computation of cosmic microwave background anisotropies in closed Friedmann-Robertson-Walker models,” *ApJ* **538**, 473–476 (2000).
31. L. Liu et al., “OmniUV: a multipurpose simulation toolkit for VLBI observation,” *AJ* **164**, 67 (2022).
32. J. Gruber, A. Nothnagel, and J. Böhm, “VieRDS: a software to simulate raw telescope data for very long baseline interferometry,” *PASP* **133**, 044503 (2021).

Jānis Šteinbergs is a research assistant at the Ventspils International Radioastronomy Centre. He is a Ventspils University of Applied Sciences Masters of Computer Science graduate. His previous work has involved in development of tools for automation of radio astronomy data processing.

Karina Šķirmante is a researcher at Ventspils University of Applied Sciences and a doctoral candidate at the University of Latvia. Her doctoral thesis focuses on advancing techniques for analyzing observational data of small planetary bodies. She possesses experience in the development of radio astronomical data processing methods and tools. Her previous work has involved the application of high-performance computing and parallel algorithms to enhance data processing efficiency and accuracy.

Artis Aberfelds is a researcher at the Ventspils International Radioastronomy Centre. He recently obtained his PhD in natural sciences (sub-field astrophysics) from the University of Latvia in March 2024. His current interests include masers, observation techniques, massive star formation, and accretion bursts.

Vladislavs Bezrukovs a researcher at the Ventspils International Radioastronomy Centre and a doctoral candidate at the University of Latvia, excels in coordinating interferometric observations at the Irbene Observatory as an EVN Friend. He actively contributes to the advancement of new technologies and software within the field. He specializes in AGN VLBI studies and single-dish monitoring as part of his personal scientific interests.

Ivar Shmeld is a leading researcher at the Astronomy and Astrophysics Department of Ventspils International Radioastronomy Centre, Ventspils University of Applied Sciences. His scientific interests include radio astronomy, interstellar medium, and astrochemistry. In recent years, he has mostly focused on maser radiation from high-mass star formation regions.

Ross A. Burns is a post-doctoral researcher at the RIKEN cluster for pioneering research in Japan. His research focuses on using radio frequency maser observations to investigate high-mass star formation. He is the principal investigator for the IVARS project and the Maser Monitoring Organisation (M2O).